SCIENTIFIC REPORTS

SUBJECT AREAS:
PARASITOLOGY
IMAGING
BIOCHEMISTRY
CELL BIOLOGY

Received
19 October 2011

Accepted
28 November 2011

Published
12 December 2011

Correspondence and requests for materials should be addressed to A.S. (amit.icgeb@gmail.com)

* These three authors have contributed equally to this work.

Uneven spread of *cis*- and *trans*-editing aminoacyl-tRNA synthetase domains within translational compartments of *P. falciparum*

Sameena Khan[1]*, Arvind Sharma[1]*, Abhishek Jamwal[1]*, Vinay Sharma[2], Anil Kumar Pole[1], Kamal Kishor Thakur[1] & Amit Sharma[1]

[1]Structural and Computational Biology Group, International Centre for Genetic Engineering and Biotechnology, New Delhi 110 067, India, [2]Department of Bioscience and Biotechnology, Banasthali Vidyapith University, Banasthali, Rajasthan 304 022, India.

Accuracy of aminoacylation is dependent on maintaining fidelity during attachment of amino acids to cognate tRNAs. *Cis*- and *trans*-editing protein factors impose quality control during protein translation, and 8 of 36 *Plasmodium falciparum* aminoacyl-tRNA synthetase (aaRS) assemblies contain canonical putative editing modules. Based on expression and localization profiles of these 8 aaRSs, we propose an asymmetric distribution between the parasite cytoplasm and its apicoplast of putative editing-domain containing aaRSs. We also show that the single copy alanyl- and threonyl-tRNA synthetases are dually targeted to parasite cytoplasm and apicoplast. This bipolar presence of two unique synthetases presents opportunity for inhibitor targeting their aminoacylation and editing activities in twin parasite compartments. We used this approach to identify specific inhibitors against the alanyl- and threonyl-tRNA synthetases. Further development of such inhibitors may lead to anti-parasitics which simultaneously block protein translation in two key parasite organelles, a strategy of wider applicability for pathogen control.

Malaria remains a major human health problem, resulting in 200–300 million human infections and ~1 million fatalities per year[1]. The extraordinarily virulent malaria parasite, *Plasmodium falciparum*, is responsible for most mortality associated with malaria[2]. As the malaria parasite and its vectors quickly develop resistance to drugs and insecticides, it is vital to continually discover new potential drug targets which can be exploited for next generation of anti-malarials[2]. Cognate aminoacyl-tRNA coupling is done by ubiquitous and essential enzymes called aminoacyl-tRNA synthetases (aaRSs). These enzymes catalyze ligation of specific amino acids to their cognate tRNAs, and this reaction proceeds in two steps. First, aaRSs activate their substrate amino acids by forming an aminoacyl-adenylate adduct. Next, the aminoacyl moiety is transferred to the CCA acceptor end of the tRNAs[3]. Clearly, a highly reliable mechanism for discrimination between cognate and non-cognate amino acid/tRNA substrates is therefore required[4]. Quality control, in terms of selecting correct amino acid versus an isosteric substrate, is implemented at several steps during protein translation to ensure faithful production of amino acid-tRNAs as encoded in the genomes[4]. A key enzymatic activity in this scheme is the proof-reading (or editing) performed by highly specific *cis*- which are often appended to aaRSs, and proof reading by *trans*- editing factors[3,5]. For example, the three class I aaRSs-isoleucyl-tRNA synthetase (IRS), leucyl-tRNA synthetase (LRS) and valyl-tRNA synthetase (VRS) have homologous editing domains called connective polypeptide 1 (CP1) which can catalyze both pre- and post- transfer substrates[3,5]. On the other hand, editing domains of class II aaRSs like in threonyl-tRNA synthetase (TRS), prolyl-tRNA synthetase (PRS), alanyl-tRNA synthetase (ARS) and phenylalanine-tRNA synthetase (FRS) are more diverse and predominantly catalyze post-transfer hydrolysis of misacylated tRNAs. Further, free standing editing domains like YbaK and alanine-tRNA synthetase editing domain homolog (AlaX) maybe required for *trans*-editing of mischarged tRNAs[3,5]. At times when aaRSs fail to exclude D-amino acids during charging of cognate tRNAs, a widely distributed *trans*- editing domain called D-tyrosyl-tRNA deacylase (DTD) implements enantiomeric selectivity control. The editing ability of *P. falciparum* DTD was earlier shown to be an essential activity for parasite survival[6,7]. In higher eukaryotes like mice, editing-defective alanyl-tRNA synthetase can lead to protein misfolding in neurons and eventual neurodegeneration[8], highlighting the premium on proofreading abilities in protein translation process.

We have earlier shown that *P. falciparum* encodes for a total of 36 aaRSs assemblies[9], a number significantly less than the ~60 expected if all three parasite compartments (apicoplast, mitochondria and the cytoplasm) had each ~20 aaRSs. In this study, we have used multi-disciplinary approaches to spatially map the overall distribution of eight putative *cis*- and one *trans*- editing domain from *P. falciparum.* Our data reveal a strikingly asymmetrical spread of proofreading domains between the parasite apicoplast and cytoplasm. We show that of the eight putative editing domain containing aaRSs in *P. falciparum,* the single copy alanyl- (Pf-Ed-ARS) and threonyl-tRNA synthetases (Pf-Ed-TRS) are dual targeted to apicoplast and cytoplasm. Small molecule-based inhibition of either the editing or aminoacylation activities of Pf-Ed-ARS or Pf-Ed-TRS can therefore provide a unique focus for blocking protein translation in all parasite compartments simultaneously.

Results

***P. falciparum* possesses eight putative editing modules.** We earlier showed that the genome sequence of *P. falciparum* encodes 36 aminoacyl-tRNA synthetase assemblies (aaRSs) of roughly equivalent predicted distribution between apicoplast and cytoplasm[9]. Our present in-depth computational probing of domain and sub-domain structures within the 36 aaRSs has revealed eight putative *cis*-editing domains in *P. falciparum* aaRSs, which seem to retain the critical residues necessary for hydrolysis activity associated with editing domains (Fig. 1). To establish a nomenclature, Pf aaRSs which contain *cis*- and *trans*- editing domains are noted in this paper as Pf-Ed-aaRSs (for example, Pf-Ed-ARS). We have investigated and summarized the conserved residues and motifs within canonical, active editing domains in *P. falciparum* (Fig. 1). The varying specificities of aaRSs for isosteric amino acids (potential errors) are also depicted, along with relevant names for the editing domains (Fig. 1). The eight Pf aaRSs that contain *cis*-editing domain/factors (Pf-Ed) belong to class I aaRSs: [Pf-Ed-IRS1, Pf-Ed-IRS2, Pf-Ed-LRS, Pf-Ed-VRS], class II aaRSs: [Pf-Ed-ARS, Pf-Ed-FRS, Pf-Ed-PRS and Pf-Ed-TRS]. An independent *trans*- editing enzyme called Pf-DTD is also encoded in the parasite genome (Fig. 1). Our analysis suggests that aaRSs for amino acids like isoleucine, leucine, valine, phenylalanine and proline are present in at least 2 copies (likely one each for protein translation in apicoplast and cytoplasm, *P. falciparum* contains 3 copies of FRS). Of the two isoforms for many aaRSs, the cytoplasmic versions of Pf-Ed-IRS1, Pf-Ed-LRS, Pf-Ed-VRS, Pf-Ed-FRS, Pf-Ed-PRS possess canonical *cis*-editing domains (Fig. 1) while the apicoplast destined second copies for Pf-VRS, Pf-LRS and Pf-FRS and Pf-PRS seem to lack discernible, canonical, editing modules (Fig. 1). The only exception in this is for the amino acid isoleucine, where both the apicoplast and the cytoplasmic versions of Pf-Ed-IRS contain authentic *cis*- editing domains. Finally, *P. falciparum* encodes four single copy aaRSs – alanyl-, cysteinyl, glycyl- and threonyl-tRNA synthetases of which only the alanyl- and threonyl-tRNA synthetases seem to contain appended editing domains.

We also built atomic models for four putative editing domains from malaria parasites (Pf-Ed-LRS, Pf-Ed-IRS1, Pf-Ed-TRS and Pf-Ed-ARS) based on extensively studied homologs from non-parasitic sources where mechanistic insights and active site residues have been mapped[10–13]. Clearly, structural conservation of key participating residues that recognize and remove non-cognate amino acids provides compelling evidence that the putative editing domains from *P. falciparum* must also be functionally competent. Our modeling data suggest that Pf-Ed-LRS and Pf-Ed-IRS possess canonical class Ia editing folds and retain the key threonine and aspartate residues that confer activity on their *E. coli* and *T. thermophilus* counterparts (Fig. 1b)[10–11]. Similarly, the putative editing domains of Class II Pf-Ed-ARS and Pf-Ed-TRS contain both the classical zinc binding motifs and the pivotal active site moieties which have been delineated in well studied counterparts from *Pyrococcous horikoshii* and *E. coli* (Fig. 1b)[12–13]. These insights into putative editing domains from *P. falciparum* indicate both structural and functional conservation in terms of enzymatic editing activities.

In addition to *cis*- forms of proofreading factors in aaRSs, most organisms also possess *trans*- editing domains which are free standing enzymes[5]. These include the so-called YbaK, AlaX, ProX, TRS-Ed and DTD enzymes[5]. The Ybak domain clears mis-charged adducts like Ala-tRNA^{Pro} and Cys-tRNA^{Pro} while ProX hydrolyzes Ala-tRNA^{Pro}. Similarly, Ser-tRNA^{Ala}, Gly-tRNA^{Ala} and Ser-tRNA^{Thr} hydrolysis is catalyzed by AlaX and TRS-Ed, respectively. DTD prevents D-amino acid introduction into the translational machinery by hydrolyzing D-aa-tRNA^{aa5-7}. We failed to identify homologs of these 5 factors in *P. falciparum*, except for the already detailed DTD enzyme[6–7]. Our computational investigations however revealed that *P. falciparum* contains a variant of typical WRS (tryptophanyl-tRNA synthetase) in which parasite WRS is fused with a distant homolog of free-standing, proofreading factor called AlaX. In addition, we found a YbaK homolog appended to the *P. falciparum* prolyl-tRNA synthetase (Fig. 1). No homologs were found for ProX and TRS-ed *trans*-editing factors. Therefore, of the 5 expected *trans*- editing factors, *P. falciparum* seems to encode only three (DTD, AlaX and Ybak), where two of the latter are found fused to cytoplasmic versions of tryptophanyl-tRNA synthetase and prolyl-tRNA synthetases respectively.

Mapping of typical *cis*- and *trans*-editing containing aaRSs. We studied the subcellular localization of eight putative *cis*- editing domains (and in addition of the *trans*- factor DTD) using specific antibodies that were generated against highly pure, recombinant parasite proteins. These polyclonal antibodies were generated in mice and rabbits against highly conserved domains/regions of aaRSs (details are available in Table 1). We discovered differential localization of several aaRSs (in terms of apicoplastic or cytoplasmic residency) when tested in the asexual stages of parasite growth (Fig. 2). For brevity, only the late ring and early trophozoite-stage localizations are depicted here but patterns were identical in other intra-erythrocytic stages (Fig. 2). All canonical class I and class II editing domain-containing aaRSs were predicted to be in the parasite cytosol, except for Pf-Ed-IRS2 which was recently shown to be targeted to the parasite apicoplast based on GFP-fused Pf-Ed-IRS2[14]. The cytoplasm localized enzymes showed a non-punctuate, broadly spread, uniformly distributed staining in the parasites, as judged by visual analyses and volumetric examination of z-stacks by confocal microscopy (Fig. 2). Several computational predictions for aaRS localization were not confirmed by our experimental analyses once probing was done using protein-specific antibodies. For example, PF-Ed-IRS2, PF-Ed-ARS, PF-Ed-TRS were predicted to be both in parasite apicoplast and the nucleus using PATS[15] and NLS[16] programs respectively. However, as shown (Fig. 2b, 3a and 4a) none of the three PF-Ed-IRS2, PF-Ed-TRS, PF-Ed-ARS enzymes reside in the parasite nucleus. Encouragingly, PATS predictions were generally verified by our experimental microscopy data. Finally, Pf-DTD was re-tested for possible localization in parasite apicoplast (Fig. 2g), and we confirm it to be in solely sequestered in the parasite cytoplasm[6,7]. Absence from malaria parasite mitochondria of the 9 editing factors tested in this study (based on confocal IFA) suggests mitochondrial reliance on alternate pathways such as import of aminoacylated tRNA, a strategy used by many organisms[17].

Expression and targeting of single copy Pf-Ed-ARS and Pf-Ed-TRS. Of the four (alanyl-, cysteinyl, glycyl- and threonyl-tRNA synthetases) single copy *P. falciparum* aaRSs, only alanyl- and threonyl-tRNA synthetases enzymes possess canonical editing domains to guard against Ser/Gly-tRNA^{Ala} and Ser-tRNA^{Thr} respectively (Fig. 1). We interrogated the spatial distribution of these single copy Pf-Ed-ARS and Pf-Ed-TRS within the parasite using

a

Classa	Name of aaRS	Editing substrate	Copy No.	Plasmodb ID	Predicted localization	Conserved *cis*-editing domain features	Conserved *trans*-editing factor
Class I	Pf-Ed-IRS1	Val	2	PF13_0179	Cy	CP1/Thr rich motif	-
	Pf-Ed-IRS2			PFL1210w	Ap & Nu	CP1/Thr rich motif	-
	Pf-Ed-LRS	Val, Met, Ile	2	PFF1095w	Cy	CP1/Thr rich motif	-
	Pf-LRS			*Pf08_0011	Ap & Nu	-	-
	Pf-Ed-WRS	Gly, Ser	2	PF13_0205	Cy	AlaX	-
	Pf-WRS			*PFL2485c	Ap	-	-
	Pf-Ed-VRS	Thr	2	PF14_0589	Cy	CP1/Thr rich motif	-
	Pf-VRS			*PFC0470w	Ap	-	-
Class II	Pf-Ed-ARS	Gly, Ser	1	PF13_0354	Ap & Nu	HXXXH and CXXXH	-
	Pf-Ed-FRS	Tyr, Ile	2	PF11_0051	Cy	B3 and B4	-
	Pf-FRS			*PFL1540c	Ap	-	-
	Pf-Ed-PRS	Ala, Cys	2	PFL0670c	Cy	YbaK	-
	Pf-PRS			* PFI1240c	Ap & Nu	-	-
	Pf-Ed-TRS	Ser	1	PF11_0270	Ap & Nu	HXXXH and CXXXH	-
Trans-editing protein	Pf-DTD	D amino acid	1	PF11_0095	Cy	-	D-tyrosyl-tRNA^{Tyr} deacylase

b

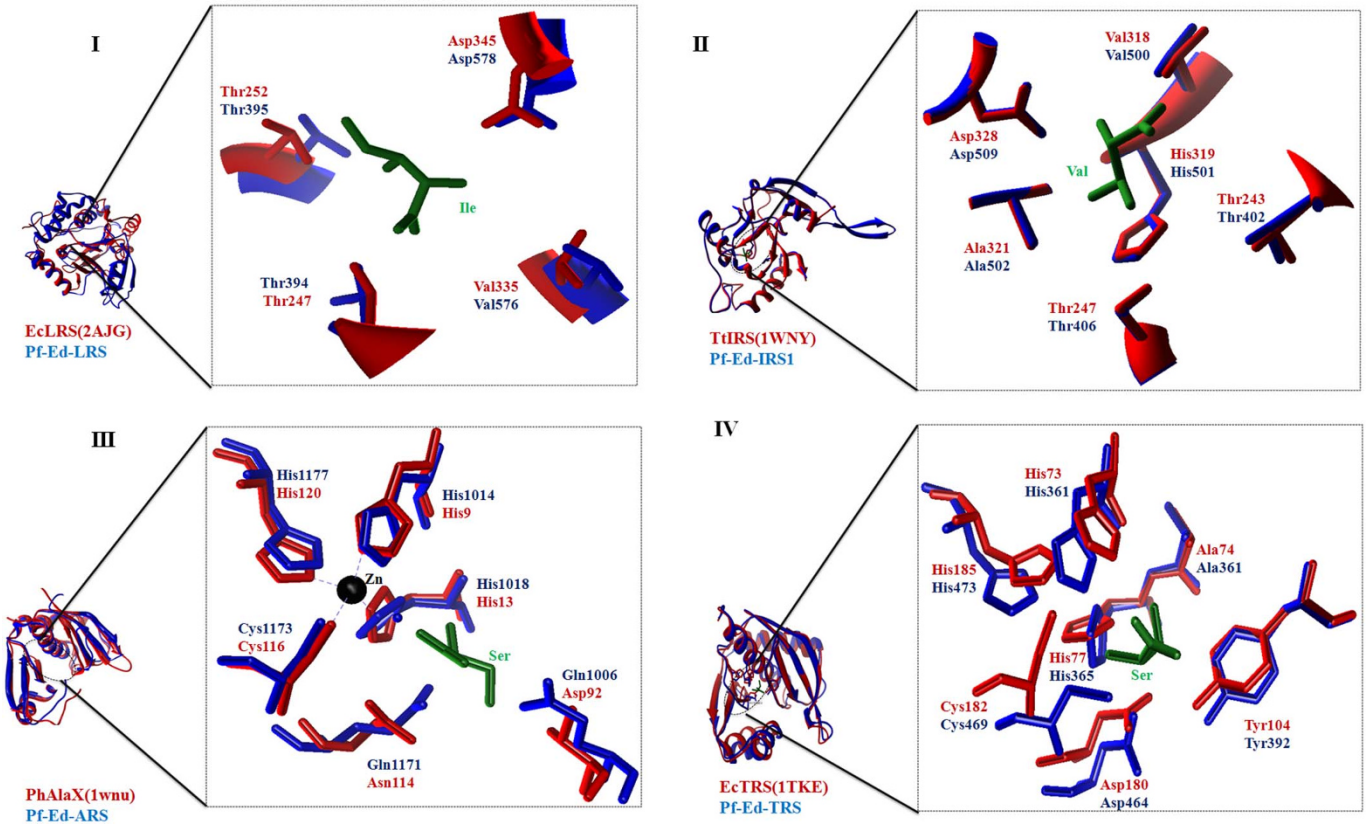

Figure 1 | Distribution of putative editing domains in *P. falciparum*. (a) Total number of *P. falciparum* putative editing-domain containing aaRSs, their amino acid specificities, their domain signatures and predicted localizations. Symbol * denotes the canonical *P. falciparum* aaRSs which lack discernible, typical editing domains. These were not investigated further in this work. (b) I, II, III, IV show active site architect of putative editing domains of Pf-Ed-LRS, Pf-Ed-IRS1, Pf-Ed-ARS and Pf-Ed-TRS showing the high level of conservation in critical residues involved in catalysis. PDB IDs are enclosed in brackets.

specific antibodies against editing domains of each. Earlier, our bioinformatics-based annotation had suggested co-localization of Pf-Ed-ARS and Pf-Ed-TRS in parasite nucleus and apicoplast (using PATS and NLS servers). Once again, the NLS server mis-predicted targeting, and based on immunofluorescence experiments we concluded that Pf-Ed-ARS and Pf-Ed-TRS compartmentalize in apicoplast and cytoplasm. In these studies, the parasites were co-stained with DAPI and we failed to observe any overlap of fluorescence emanating due to the protein detection, indicating absence of Pf-Ed-TRS and Pf-Ed-ARS from the parasite nucleus (Fig 3a, 4a). Besides the more obvious cytosolic signal in confocal assays, which convincingly overlapped with the known cytoplasmic marker Pf-DTD, a clear overlay was evident between Pf-Ed-ARS and Pf-Ed-TRS fluorescence and apicoplastically resident GFP indicating transit of Pf-Ed-TRS and Pf-Ed-ARS to this organelle (Fig. 3b, 4b). Confocal IFAs with pre-immune sera and anti-histidine tag also failed to produce fluorescence validating the specificity of Pf-Ed-TRS and Pf-Ed-ARS antibodies used (Fig. 3b, 4b). Competitive confocal IFAs, where antibodies were pre-incubated with their respective proteins (Pf-Ed-TRS and Pf-Ed-ARS) at varying molar concentrations, again revealed lack of fluorescence signals thereby confirming the specificities of antibodies used in this work (Fig. 3c, 4c). Two confocal imagery-based movies (supplementary movie S1 and supplementary movie S2) which show bi-compartmentalization

Table 1 | Detailed description of cloning, expression and purification of nine *cis*- and *trans*-editing domains from *P. falciparum*.

Enzyme	PlasmoDB ID	Protein length(aa)	Cloning sites	Cloning vector(EMBL)	Expression strain	Induction	Buffer used	Resin used	Purification method
Pf-Ed-IRS1	PF13_0179	388–577	5′NcoI-3′KpnI	pETM-41	B834(DE3)	Culture was induced with IPTG (0.5 mM at OD of 0.6), and growth was continued for O/N at 18°C	Lysis buffer-20 mM Tris (7.4), 200 mM NaCl, 10% glycerol, 10 mM βME Elution buffer-10 mM Maltose in lysis buffer	Amylose resin	Superdex S-200 gel filtration chromatography (Amersham Biosciences).
Pf-Ed-IRS2	PFL1210w	551–800	5′NcoI-3′KpnI	pETM-41	B834(DE3)	Culture was induced with IPTG (0.5 mM at OD of 0.6), and growth was continued for O/N at 18°C	Lysis buffer-20 mM Tris (7.4), 200 mM NaCl, 10% glycerol, 10 mM βME Elution buffer-10 mM Maltose in lysis buffer	Amylose resin	Superdex S-200 gel filtration chromatography (Amersham Biosciences).
Pf-Ed-LRS	PFF1095w	367–694	5′NcoI-3′KpnI	pETM-41	B834(DE3)	Culture was induced with IPTG (0.5 mM at OD of 0.6), and growth was continued for O/N at 18°C	Lysis buffer-20 mM Iris (7.4), 200 mM NaCl, 10% glycerol, 10 mM βME Elution buffer-10 mM Maltose in lysis buffer	Amylose resin	Superdex S-200 gel filtration chromatography (Amersham Biosciences).
Pf-Ed-VRS	PF14_0589	254–407	5′NcoI-3′KpnI	pETM-11	BL21-DE3	Culture was induced with IPTG (0.5 mM at OD of 0.6), and growth was continued for 4 hours at 18°C	Lysis buffer-20 mM Tris (8.0), 500 mM NaCl, 10% glycerol, 10 mM βME Elution buffer-20 mM Immidizaole in lysis buffer	Ni-NTA beads (Qiagen)	Superdex S-75 gel filtration chromatography (Amersham Biosciences).
Pf-Ed-ARS	PF13_0354	998–1234	5′NcoI-3′KpnI	pETM-11	BL21pLysS	Culture was induced with IPTG (1 mM at OD of 0.6–0.8), and growth was continued for O/N at 18°C	Lysis buffer-20 mM Tris (8.0), 500 mM NaCl, 10% glycerol, 10 mM β ME Elution buffer-20 mM Immidizaole in lysis buffer	Ni-NTA beads (Qiagen)	N/A
PF-Ed-FRS	PF11_0051	1–623	5′NcoI-3′KpnI	pETM-11	BL21-DE3	Culture was induced with (0.5 mM IPTG at O.D. of 0.8) and growth was continued for O/N at 18°C	Lysis buffer-20 mM Tris, 300 mM NaCl, 20 mM Imidaole (pH 8), Elution buffer-increasing concentration of imidazole (upto 500 mM)	Ni-NTA beads (Qiagen)	N/A
Pf-Ed-TRS	PF11_0270	352–528	5′NcoI-3′KpnI	pETM-11	BL21pLysS	Culture was induced with IPTG (1 mM at OD of 0.6–0.8), and growth was continued for O/N	Lysis buffer-20 mM Tris (8.0), 500 mM NaCl, 10% glycerol, 10 mM βME Elution buffer 20 mM Immidizaole	Ni-NTA bea ds (Qiagen)	N/A
Pf-Ed-PRS	PFL0670c	1–746	5′NcoI-3′KpnI	pETM-30	B834(DE3)	Culture was induced with IPTG (0.5 mM at OD of 0.6), and growth was continued for O/N at 18°C	Lysis Buffer-20 mM Tris, 300 mM NaCl, Imidazole, 20 mM Imidazole (pH 8). Elution buffer-increasing concentration of imidazole (upto 500 mM)	Ni-NTA beads (Qiagen)	Superdex S-200 gel filtration chromatography (Amersham Biosciences).
Pf-DTD	PF11_0095	1–164	5′NcoI-3′KpnI	pET-28a	B834(DE3)	Culture was induced with IPTG (0.5 mM at OD of 0.6), and growth was continued for 5 h at 37°C	Lysis buffer-50 mM NaH2PO4, 300 mM NaCl, 20 mM imidazole, pH 7.3 Elution buffer-increasing concentrati on of imidazole (up to 500 mM).	Ni-NTA beads (Qiagen)	Superdex S-75 gel filtration chromatography (Amersham Biosciences).

of alanyl- and threonyl-tRNA synthetases respectively have been uploaded with this manuscript. These data together suggest that the parasite has developed a dual transport strategy to make available the same copy of Pf-Ed-ARS and Pf-Ed-TRS in two of its translationally active compartments. This bi-location ensures that the parasite has access not only to aminoacylation activities for alanines and threonines, but also to *cis*-editing factors within Pf-Ed-ARS and Pf-Ed-TRS that impose further translational governance. The protein expression profiles of Pf-Ed-TRS and Pf-Ed-ARS in parasite lysates consistently showed two bands for each (Fig. 3a, 4a). On SDS-PAGE, Pf-Ed-TRS migrated as a doublet of ~120 kDa (expected) and 70 kDa (processed) while Pf-Ed-ARS migrated at ~165 kDa (expected) and at ~110 kDa (processed) (Fig. 3a, 4a). For both these enzymes, we had produced antibodies against their putative editing domains (see Table 1). Therefore, antibody recognition and molecular weights of the processed smaller bands for Pf-Ed-ARS and Pf-Ed-TRS together argue for existence of variants of Pf-Ed- Pf-Ed-TRS and ARS in *P. falciparum* that retain aminoacylation and the editing domains (Fig. 3a, 4a).

Three-dimensional modeling and inhibitor dockings. A multiple sequence alignment of *P. falciparum* and related eukaryotic alanyl- and threonyl-tRNA synthetases revealed, expectedly, a number of sequence insertions in parasite enzymes. These alignments also showed conservation in aminoacylation motifs (motif-1, motif-2, and motif-3) and homology within the two editing site motifs (HXXXH and CXXXH). We therefore structurally modeled Pf-Ed-ARS (Fig. 4d) and Pf-Ed-TRS enzymes based on crystal structures of available homologs from the PDB database. Homology search using PSI-BLAST resulted in templates for both ARS (PDB ID: 1YFR) and TRS ([PDB ID: 1QF6) with significant sequence identity in each case. Using these reliably built atomic models, we screened small molecule libraries seeking compounds that docked into Pf-Ed-ARS and Pf-Ed-TRS aminoacylation sites. The top scoring compounds made n-π and π-π interactions with arginines and phenylalanines in TRS (F667, R651) (data not shown) and also in ARS (F482, R630) (Fig. 4e). The selected compounds were tested for anti-parasitic activities subsequently.

Growth inhibition assays using inhibitors of Pf-Ed-ARS and Pf-Ed-TRS. Structure-based *in silico* screening routines were used to provide a list of potential inhibitors against Pf-Ed-ARS and Pf-Ed-TRS. Top 6 and 11 compounds, selected for Pf-Ed-ARS and Pf-Ed-TRS, were tested against *P. falciparum* 3D7 cultures (supplementary Table S3). All 11 inhibitors which docked into the aminoacylation site of Pf-Ed-TRS showed inhibition of parasite growth but at high concentrations (data not shown). Of the 6 compounds tested for inhibition of aminoacylation activity of Pf-Ed-ARS, two compounds (A3 and A5) showed low IC_{50} values of ~90 μM (A3) and 8 μM (A5) respectively (Fig. 4f). Based on these data, we re-validated the anti-parasitic activity of compound A5 (Fig. 4g). The sets of detailed atomic interactions (based on inhibitor docking studies) between A5 and Pf-Ed-ARS provide a very useful platform to generate second generation inhibitors. All active compounds ($IC_{50} \leq 100$ μM, i.e., A3 and A5) were evaluated for cytotoxicity using MTT assays against fibroblast L929 cell lines (Fig. 4h) and HeLa cells (Fig. 4i), and were found to be devoid of cytotoxicity within the range of parasite IC_{50} values.

Discussion

This study provides the first in-depth mapping of protein-based quality control mechanisms used by *P. falciparum* during protein synthesis (Fig. 5). Fidelity during protein translation, in terms of both correct cognate amino acid pairing with its tRNA, and hydrolysis of wrongly charged isosteric amino acids, is maintained through aminoacyl-tRNA synthetases (aaRSs) in conjunction with *cis*- and *trans*- editing factors[3,5]. The editing functions therefore oversee aaRS amino acid selectivity, and ensure correction of even low abundance errors in protein synthesis[4]. Proofreading by editing factors entails hydrolysis of non-cognate aminoacyl adenylates/tRNA which are bound to aaRSs[5]. For example, mischarging of $tRNA^{Ala}$ with serine or glycine will result in erroneous propagation of the genomic message, and therefore needs to be 'rectified' by hydrolysis of the mis-acylated tRNAs such that another round of aminoacylation by, in this case, alanyl-tRNA synthetase results in Ala-$tRNA^{Ala18}$. Similarly, corrections by editing domain of phenylalanyl-tRNA synthetase (FRS) will protect mis-incorporation of tyrosines where phenylalanines are meant to be, by hydrolysis of mis-charged Tyr-$tRNA^{Phe19}$. Importance of editing by aaRSs is also underscored by previous findings which show that mis-acylation can result in neurodegenerative diseases in mammals, growth defects in bacteria and in apoptosis[8,20,21]. Mischarging of tRNAs with non-cognate amino acids is also recognized as an adaptive response to withstand oxidative stress[22]. Therefore, investigations on quality controls mechanisms used during protein translation are becoming increasingly significant. This is the first experimental survey of spatial distribution of putative editing-domain containing aaRSs within the malaria parasite (Fig. 1). We did not observe localization of any of the 9 editing modules in the parasite mitochondria. It has been shown previously[23] that *P. falciparum* apicoplast is translationally active (although the same has not been shown for parasite mitochondria but must be so) indicating that the disparate compartments within parasite walls must all have access to the basic translation machinery.

The malaria parasite apicoplast, a distant relative of non-photosynthetic plastids, translates up to 30 proteins within its compartment[24]. It therefore requires a full complement of functioning aaRSs, possibly replete with factors responsible for proofreading. Using multi-disciplinary techniques, we show that two of the three major sites of protein translation in *P. falciparum* each likely harbor ~20 aaRSs, of which at least two single copy enzymes, in the form of alanyl- and threonyl-tRNA synthetases are bi-localized. Further, our genome-wide *cis*- and *trans*-proofreading domain mappings reveal that the apicoplast lacks several translational error correction modules (Fig. 2 a–g). One such exception is in case of amino acid isoleucine. Intra-erythrocytic malaria parasite growth is dependent on import from extracellular medium of several nutrients, but critically of the amino acid isoleucine, which is missing from adult hemoglobin whose breakdown provides most other amino acids[25]. A quick survey of the ~30 proteins translated in apicoplast suggests that ~17% of constituent residues are isoleucines. Therefore, it is likely that the apicoplast organelle, while dispensing with need for proofreading domains from several other aaRSs, is still reliant on an active editing factor, via apicoplastic PF-Ed-IRS CP1 editing domain, which will for instance clear the mischarged Val-$tRNA^{Ile}$. Indeed, it has been considered that some aaRSs which lack canonical editing domains are inherently less prone to mis-acylation[5]. Species-specific variations in genomes of organisms, in terms of retaining or foregoing error-correction modules in protein translation, are clearly of tremendous significance for understanding protein translation and fidelity governance. Our present work suggests that the apicoplast-bound *P. falciparum* aaRSs (Pf-LRS, Pf-VRS, Pf-FRS and PF-PRS) seem to lack discernible, canonical editing domains based on absence of key signature motifs. In line with this, several studies from other eukaryotes have previously shown that mitochondrial versions of aaRSs can encode non-functional editing domains[26,27]. Finally, we also observed that the *trans*-editing factor DTD, which is both ubiquitous and required for cell grown in parasite and bacteria[6,28], is absent from parasite apicoplasts. Taken together, these data strongly argue that the apicoplast-based protein translation is not, besides correct charging of isoleucine onto its cognate tRNA, overly dedicated towards proofreading of mischarged Val-$tRNA^{Leu}$, Met-$tRNA^{Leu}$, Ile-$tRNA^{Leu}$, Thr-$tRNA^{Val}$, Tyr-$tRNA^{Phe}$, Ile-$tRNA^{Phe}$, Ala-$tRNA^{Pro}$ and Cys-$tRNA^{Pro}$. Apart from aaRSs with *cis*-editing factors, many

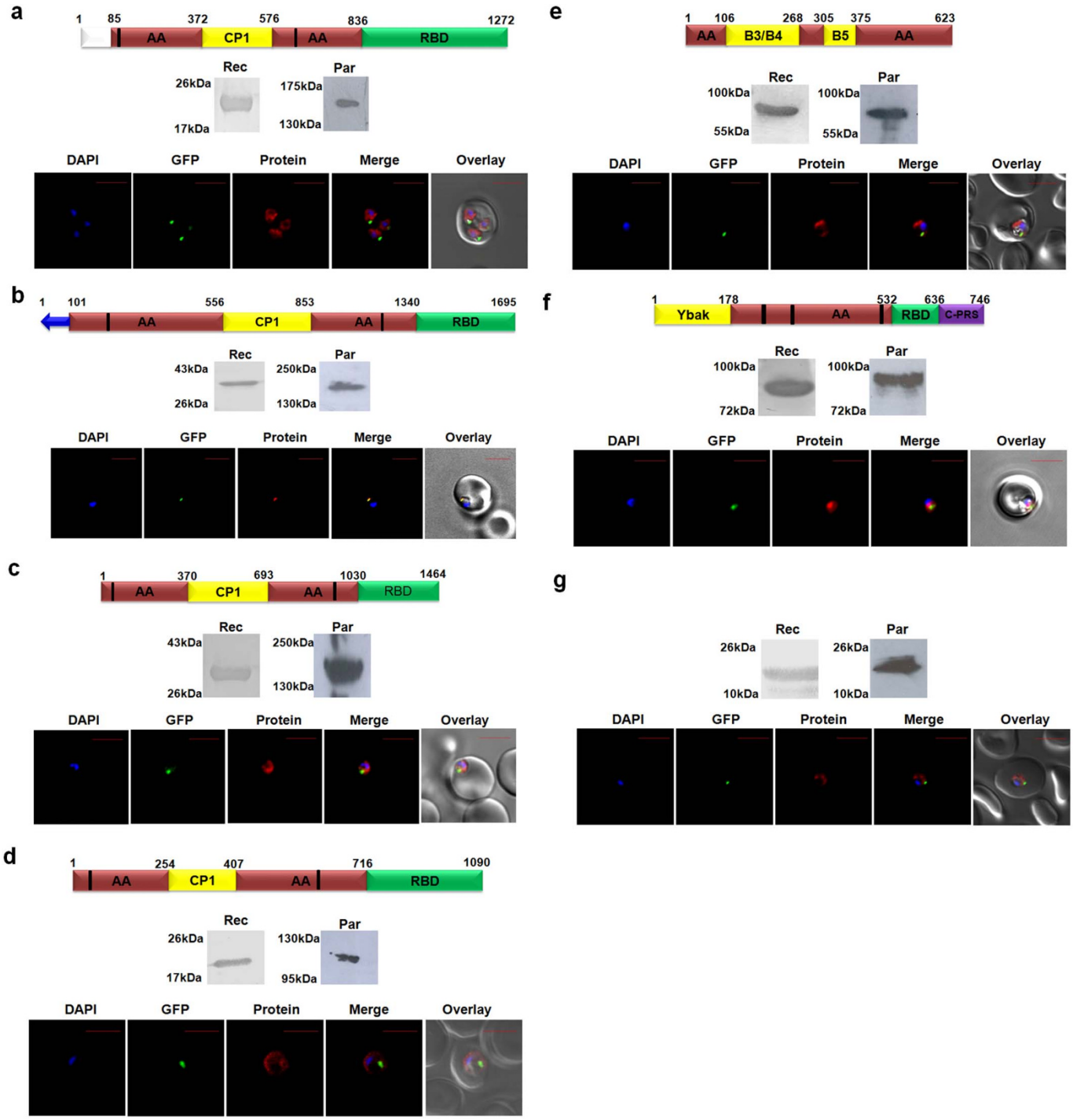

Figure 2 | Targeting of *P. falciparum* aaRSs and of DTD. Localization of (a) Pf-Ed-IRS1 (b) Pf-Ed-IRS2 (c) Pf-Ed-LRS (d) Pf-Ed-VRS (e) Pf-Ed-FRS (f) Pf-Ed-PRS (g) Pf-DTD. In all cases, upper panels show name of *P. falciparum* aminoacyl-tRNA synthetase, and their domain/ subdomain features. Middle panels show *P. falciparum* aminoacyl-tRNA synthetase expression in parasites (Par) and detection of recombinant *P. falciparum* aminoacyl- tRNA synthetase domains (Rec) by western blot analysis. Lower panels display their cellular localizations. Editing domains are colored yellow, aminoacylation domain (AA) is in red; RNA binding domain (RBD) is in green; ProRS specific C-terminal domain is in purple and un-annotated domains are in white. Blue arrow represents apicoplast targeting sequences predicted by PATS. Conserved motifs are highlighted by black strips. The parasite line used was GFP-tagged (strain D10 ACP_{leader}-GFP) where apicoplast fluorescence is in green. DAPI staining is in blue while aminoacyl-tRNA synthetases are stained with Alexa594 (red).

organisms also code for independent modules such as AlaX, ProX, Ybak, and TRS-ed[3,5]. It is well appreciated that serine-glycine toxicity, resulting from mis-charging of $tRNA^{Ala}$ with these amino acids rather than with alanine, is a major challenge for any cell. This is partly due to the inherent misrecognition of serine/glycine by alanyl-tRNA synthetases, which are therefore highly susceptible to charging $tRNA^{Ala}$ with Ser/Gly instead of Ala[18]. Indeed, small defects in the editing domain of alanyl-tRNA synthetases have been linked to neuro-degeneration[8]. Apparently, the poor discrimination between serines/glycines and alanines is of severe consequences in biology, and therefore an additional check-point in the form of AlaX *trans*-editing factors have evolved[18]. AlaX is thus a backup proofreading

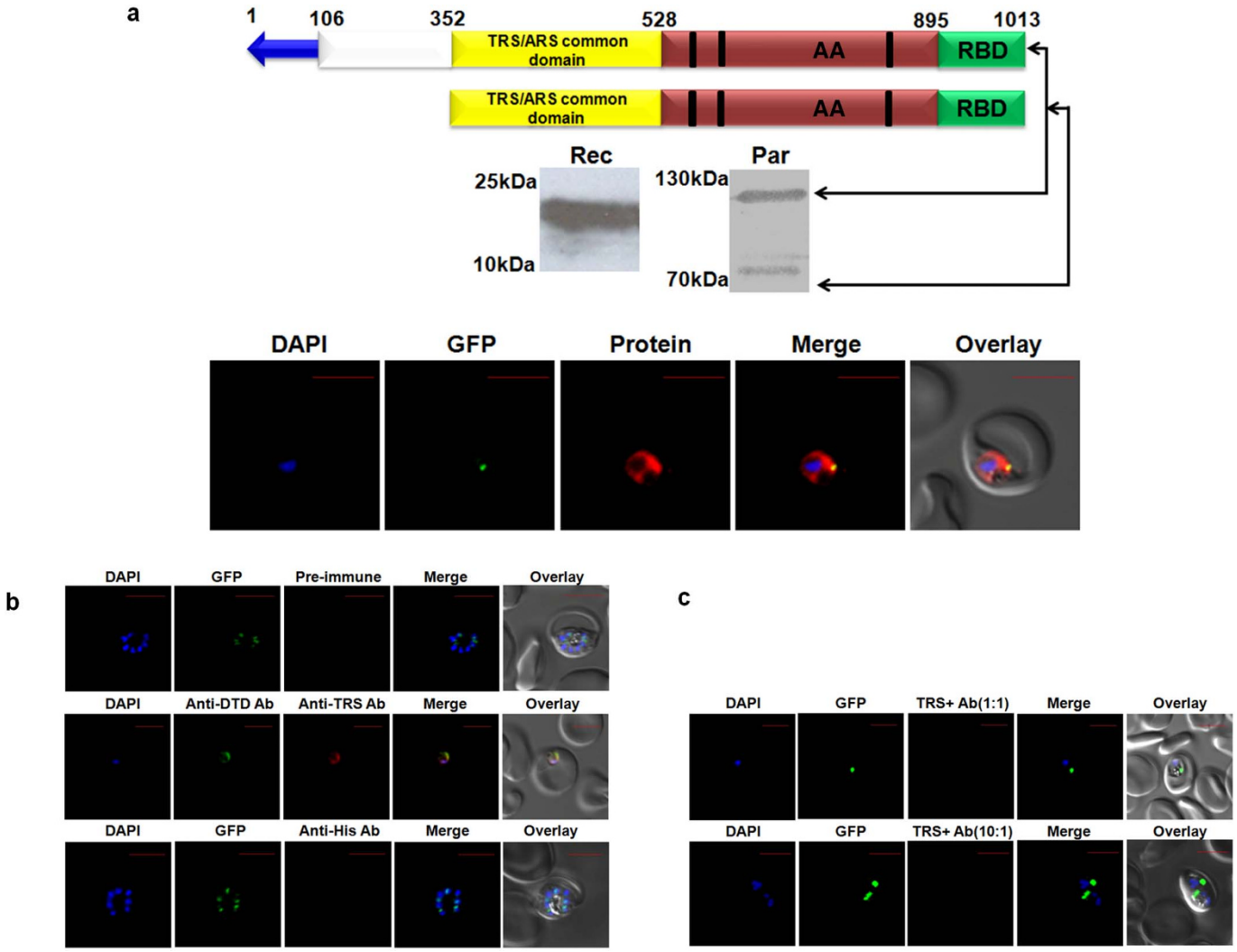

Figure 3 | Expression and localization of Pf-Ed-TRS. (a) Upper panel shows *P. falciparum* aminoacyl-tRNA synthetase name, and domain/ subdomain features. Middle panel shows *P. falciparum* aminoacyl-tRNA synthetase expression in parasites (Par) and detection of recombinant *P. falciparum* aminoacyl- tRNA synthetase domains (Rec) by western blot analysis. Lower panel displays their cellular localizations. Editing domains are colored yellow, aminoacylation domain (AA) is in red; RNA binding domain (RBD) is in green. Blue arrow represents apicoplast targeting sequences predicted by PATS. Conserved motifs are highlighted in black strips. (b) Upper and lower panels show confocal IFA with pre-immune sera and with anti-histidine antibodies, whereas the middle panels depict cytoplasmic staining of Pf-DTD. (c) Upper and lower panels show results of competitive confocal IFAs with rabbit anti-Ed-TRS antibodies which were pre-incubated with Ed-TRS in molar ratios of 1 : 1 and 10 : 1 respectively.

solution for when insufficient quality control is displayed by alanyl-tRNA synthetases in clearing Ser/Gly-tRNA^{Ala29}. Interestingly, we discovered that such a redundant, *trans*-editing factor that covers for alanyl-tRNA synthetase is present in fusion with a seemingly canonical trypthophanyl-tRNA synthetase in *Plasmodium falciparum*. More intriguingly, this highly unusual gene fusion seems almost completely (barring one alga) confined to parasitic organisms in alveolates. Whether this unique gene fusion in pathogenic organisms confers upon them a special advantage remains to be determined.

P. falciparum encodes two single copy, canonical editing domain containing enzymes in the form of alanyl- and threonyl-tRNA synthetases. We found both of these in the parasite apicoplast as well as in the cytoplasm, revealing (1) mechanisms for bipolar targeting of some aminoacyl-tRNA synthetases in malaria parasites, and (2) parasite strategy for achieving a full complement of aminoacyl-tRNA synthetases in each of its translationally active divisions. The molecular mechanism of alanyl- and threonyl-tRNA synthetase bi-localization is not clear (their genes lack introns), however protein expression data clearly show processing of full length threonyl and alanyl-tRNA synthetases in two forms – (a) one which seems to retain most of the predicted protein, and (b) one with a significantly smaller protein which lacks the signal peptide (SP) and a subsequent un-annotated domain but retains aminoacylation activity and editing domains (Fig. 3a, 4a). This dual delivery of threonyl and alanyl-tRNA synthetases allows both the apicoplast and cytoplasm to access aminoacylation and editing activities (Fig. 3a, 4a) from single copy genes. However, this apparently clever parasite strategy also presents a window for development of specific inhibitors which if targeted against editing and aminoacylation sites of threonyl and alanyl-tRNA synthetases should block protein translation in both parasite compartments simultaneously. We decided to probe parasites' apparent Achilles' heel using inhibitors identified through structure-based inhibitor docking studies. Although the total number of compounds tested remains small, a clearly useful starting point is provided by inhibitor labeled A5 (4-{2-nitro-1-propenyl}-1,2-benzenediol). These data therefore validate the strategy of inhibiting non-redundant and spatially displaced threonyl and alanyl-tRNA synthetases in malaria parasites.

A diminished ability to proofread errors that may occur during tRNA charging, which may potentially lead to mutations, may not be

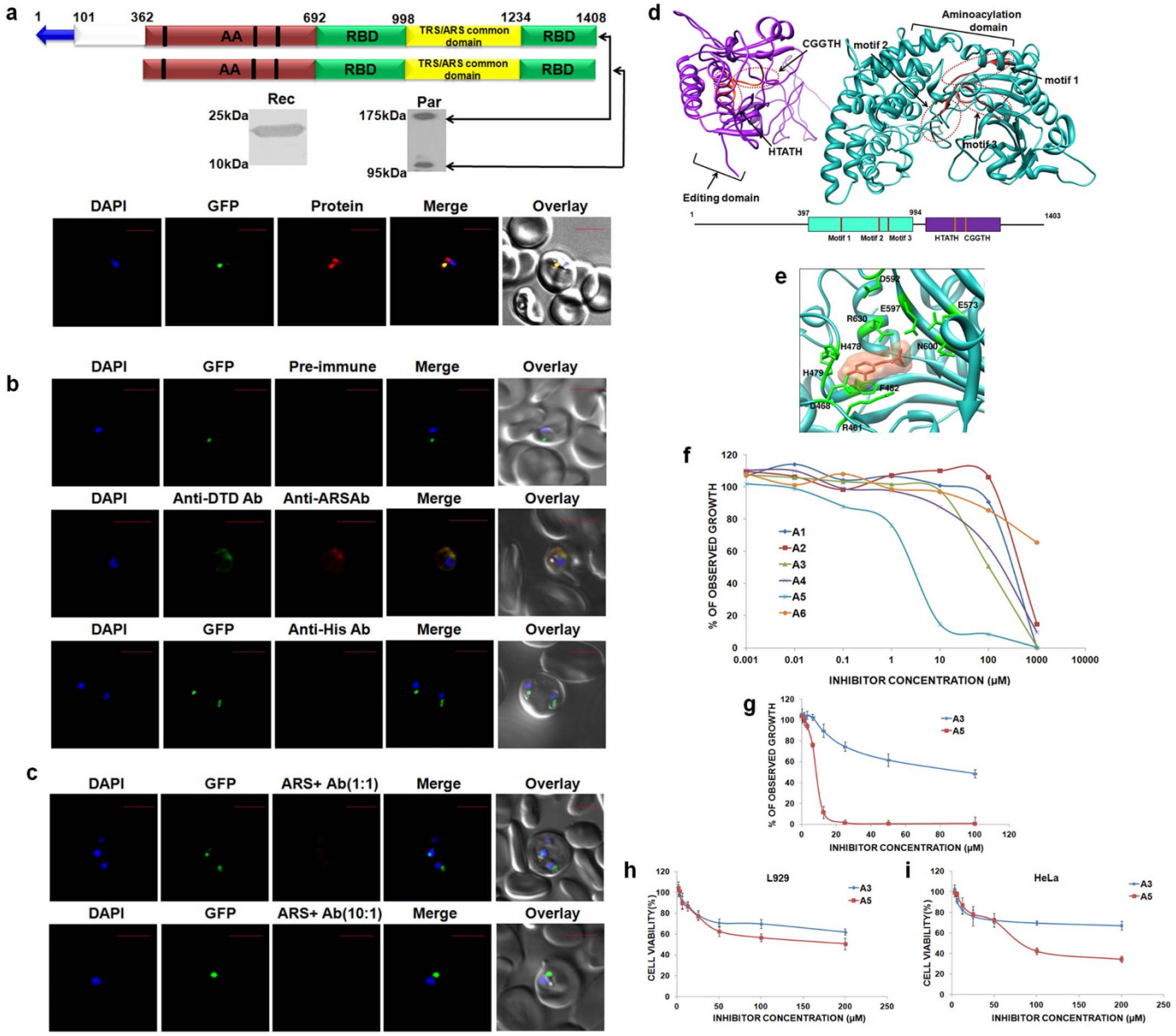

Figure 4 | Expression, localization, modeling and inhibitor screening for Pf-Ed-ARS. (a) Upper panels show *P. falciparum* aminoacyl-tRNA synthetase name, domain/ subdomain features. Middle panels show *P. falciparum* aminoacyl-tRNA synthetase expression in parasites (Par) and detection of recombinant *P. falciparum* aminoacyl- tRNA synthetase domains (Rec) by western blot analysis. Lower panels display their cellular localizations. The parasite line used was GFP-tagged (strain D10 ACP_{leader}-GFP) where apicoplast fluoresces green. DAPI staining is in blue while aminoacyl-tRNA synthetases are stained with Alexa594 (red). Editing domains are colored yellow, aminoacylation domain (AA) in red; RNA binding domain (RBD) is in green and the unidentified domain is colored in white. Blue arrow represents apicoplast targeting sequences predicted by PATS. Conserved motifs are highlighted in black strips. (b) Upper and lower panels show confocal IFA with pre-immune sera and with anti-histidine antibodies, whereas the middle panel depicts cytoplasmic staining of Pf-DTD. (c) Upper and lower panel show results of competitive IFAs with rabbit anti-Ed-ARS antibodies which were pre-incubated with Ed-ARS in molar ratios of 1 : 1 and 10 : 1 respectively. (d) Pf-Ed-ARS model with aminoacylation (AA) and editing domains (ED). The corresponding primary sequence domain structure is shown at bottom. AA motifs 1, 2 and 3 and ED motifs HXXXH and CXXXH are noted with red circles. (e) Pf-Ed-ARS-A5 inhibitor complex showing the docking of A5 within the aminoacylation domain of alanyl-tRNA synthetase. (f) Parasite growth inhibition assays using inhibitors (A1–A6, concentration range 1 nM to 1 mM) identified based on modeling of 3D structure. (g) IC_{50} value calculation of A3 and A5 compounds by using two fold dilutions of the same compounds. (h–i) Cytotoxicity activity measurements using MTT assay in concentration range of 1 μM–200 μM.

as detrimental in the parasite apicoplast system. This may be a function of both generally low error rates in aminoacylation reactions (errors rate vary ~1 in 10^3–10^4)[30], coupled with the rather small number of proteins that require translation within the parasite apicoplast (~30). The stark exception to this viewpoint is for amino acid isoleucine, where clearly the apicoplast has retained error-correction abilities in the form of CP1 editing domain within its Pf-Ed-IRS2, and where the degree of accuracy in flow of information vis-à-vis isoleucine seems pertinent.

In summary, we reveal critical differences in organelle distribution of translational quality control factors in malaria parasites – an investigation which must be tested across in other pathogens for the potential insights one can expect to gain. Clearly, malaria parasites have evolved strategies for maintaining full complement of

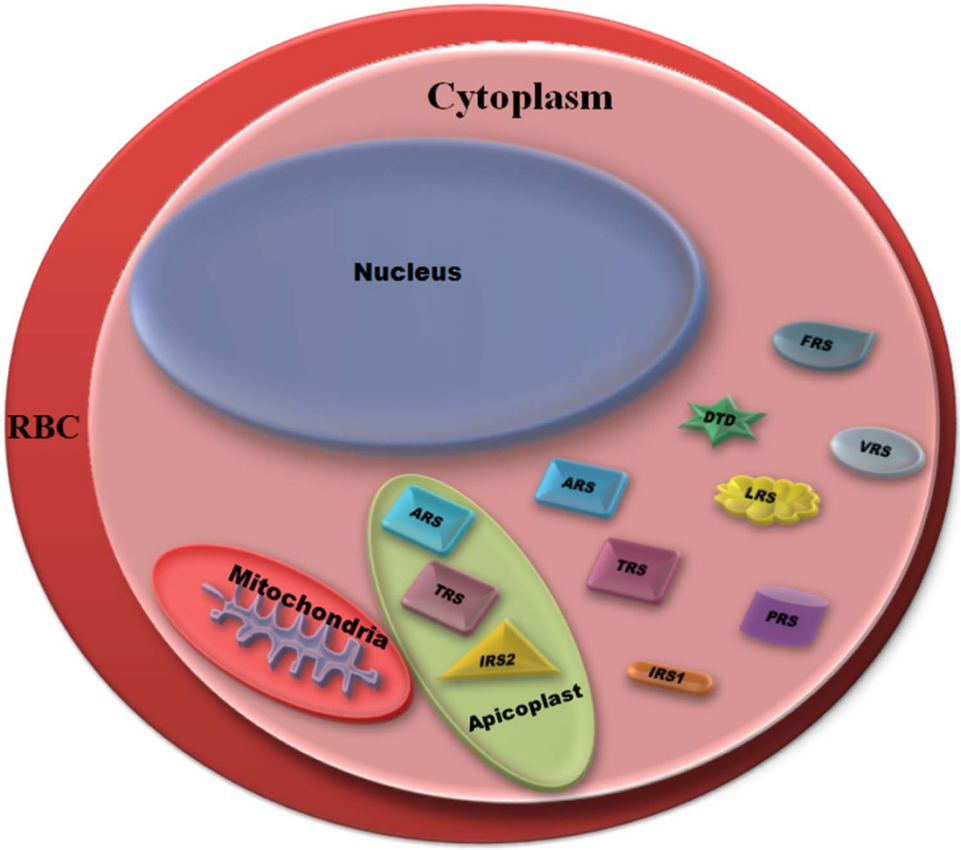

Figure 5 | Schematic illustration of *cis*- and *trans*- editing domains in *P. falciparum*. The asymmetrical distribution of proofreading activities between parasite apicoplast and its cytoplasm can be gauged by the number of editing-domain containing aminoacyl- tRNA synthetases in each compartment. The single copy Pf-Ed-ARS and Pf-Ed-TRS were found to localize both to the cytoplasm and the apicoplast.

aminoacylation, but not for proofreading activities, in its cytoplasm and apicoplast. Our comprehensive, genome-wide interrogations of proofreading factors utilized by malaria parasites during protein translation indicates (1) lack of several editing factors in apicoplastic aaRSs, (2) unusual appendage of AlaX domain to WRS, a feature apparently unique to pathogenic alveolates, (3) partitioning of single copy alanyl- and threonyl-tRNA synthetases in both apicoplast and cytoplasm to provide each cellular division their complete set of aminoacylation activities (4) utility of probing the editing and aminoacylation activities of single copy aaRSs using inhibitors that block protein translation in multiple compartments concurrently. Critical role of aminoacyl-tRNA synthetases marks them as high value targets for therapeutic development in all pathogens. Although, both aminoacylation and editing sites represent targets for specific anti-pathogen agents, the single copy, bi-localized pathogen aminoacyl-tRNA synthetases present exceptional opportunities for drug-based protein translation inhibition in multiple pathogen organelles. Such strategies therefore may provide the next generation of anti-malarials which at the outset target multiple enzymatic activities in dual locations within the parasite.

Methods

Bioinformatics and structural analysis. Protein sequences were accessed from *Plasmodium* (PlasmoDB)[31]. Additional sequences were obtained using sequence analysis softwares and servers NCBI BLAST[32]. Various protein domains, subdomain and motifs were predicted or identified using Superfamily[33], SMART[34], Pfam[35], and also by visual inspection of alignments. Prediction of signal sequences for cellular localization was performed using various available online web-servers like PATS (prediction of apicoplast targeted sequences)[15], PredictNLS (nucleus localization signal)[16]. For homology modeling, alanyl- and threonyl-tRNA synthetase sequences were used in PSI-BLAST search against PDB database[36]. COBALT[37] was used to perform alignment of query and template sequences, and a multiple sequence alignment was generated to identify insertions in *Plasmodium falciparum* aaRSs. Prior to modeling, low complexity regions were removed and modified alignments were used for model generation by MODELER[38]. Single template modeling was performed in the case of Pf-Ed-TRS whereas a multi-template modeling was required for Pf-Ed-ARS. Best models were selected based on discrete optimized protein energy (DOPE) and Modular objective function (MOF) scores. These were validated using structural analysis verification server SAVES (http://nihserver.mbi.ucla.edu/SAVES/). Finally, the models were subjected to energy minimization using prime module of Schrodinger Suite[39] to remove outliers in Ramachandran plot, and validated again using SAVES. Once aaRS three dimensional (3D) models were obtained, their active sites were analyzed visually using sequence alignments and conserved motif information. Small molecule docking studies on Pf-Ed-ARS and Pf-Ed-TRS were initiated using Prepwizard module of Schrödinger suite and the SPECS library (http://www.specs.net). Latter were prepared using Ligprep and Qikprop modules. For *in silico* screening, compounds were annotated using 10 lead-like filters derived from Lipinski's rule of five, resulting in list of ~900 compounds. High-throughput docking studies were carried out in Auto dock vina[40] and top docking poses were isolated from each output file for further analysis. High ranking ligands were selected based on docking scores, H-bond interactions with key residues in binding site, molecular size etc and further tested in biological assays.

Production of *P. falciparum* aaRSs, antibody generation and expression analysis. All clones were expressed in *E. coli* using IPTG induction system, and proteins were purified using affinity chromatography. Sample purity was checked on SDS-PAGE and more than 90% pure samples were used for antibody generation. Detailed schemes for cloning, expression and purification of all the nine *cis*- and *trans*- editing enzymes are described in (Table 1). DTD antibodies were prepared as described earlier[6]. For others, antibodies were raised against recombinant protein regions mentioned in Table 1. In all, antibodies were raised against Pf-Ed-ARS, Pf-Ed-FRS, Pf-Ed-IRS2, Pf-Ed-PRS, Pf-Ed-TRS and Pf-Ed-VRS in mice (Balbc 21) and in rabbits (NzW) for Pf-Ed-IRS1, Pf-Ed-LRS, Pf-Ed-WRS and Pf-DTD. For western blot analysis, parasites in asynchronous *P. falciparum* cultures were released from infected RBC's by 0.05% saponin lysis and pellets were washed in PBS. Parasites were lysed by 3 rounds of freeze-thawing in RIPA buffer (50 mM Tris-HCL, 150 mM NaCl, 1 mM EDTA, 1% NP40, 0.1%SDS, 1% sodium deoxycholate, pH 7.4) containing protease inhibitors cocktail. Lysates were centrifuged and supernatants were separated on SDS-PAGE. Proteins were transferred to nitrocellulose membrane and blots were probed using specific primary antibodies and secondary alkaline phosphatase conjugated antibodies (1 : 1500 dilutions). Bands were visualized using ECL detection

kit. To exclude possibility of cross reactivity between antibodies, recombinantly expressed proteins were probed using antibodies generated against related protein domains. Same antibodies were also tested against parasite lysates where they produced predominantly single bands. The specific antibodies thus used helped us conclude that the immunofluorescence-based imagery of aminoacyl tRNA synthetases is a reliable depiction of their spatial distribution within the parasites.

Parasite culture for Immunofluorescence assays. *Plasmodium falciparum* D10 ACP_{leader}-GFP transfectant line in which GFP is targeted to the apicoplast by leader peptide of acyl carrier protein (ACP)[41], was cultured in human erythrocytes (4% hematocrit) in RPMI-1640 supplemented with 0.5% AlbumaxII (Invitrogen). The parasites were synchronized with sorbitol as described previously[42].

Green fluorescence of GFP-expressing parasites was observed and captured in fixed cells using a Nikon A1R laser scanning confocal microscope. For apicoplast co-localization studies, the D10-ACP_{leader}-GFP line in which GFP is an apicoplast marker was used. Parasite cultures were processed for immunofluorescence labeling and confocal microscopy performed as described earlier[42]. Cells were washed with PBS and fixed in solution using 4% paraformaldehyde and 0.0075% glutaraldehyde in PBS for 30 min. After one wash with PBS, fixed cells were permeabilized with 0.1% Triton X-100 in PBS for 10 min. After another PBS wash, cells were treated with 0.1 mg/ml sodium borohydride in PBS for 10 min. Cells were washed once with PBS, blocked in 3% BSA/PBS for 1 h and incubated overnight at 4°C with either mice anti-protein serum (1 : 25 dilution) or rabbit anti-protein serum (1 : 100 dilution). Cells were washed three times for 10 min each with PBS and incubated with Alexaflour594-tagged anti-mouse secondary or with AlexaFluor594-tagged anti-rabbit secondary antibody for 2 h at room temperature. These were allowed to settle onto coverslips coated with poly-L-lysine (100 mg/ml), and subsequently the coverslips were washed three times in PBS, mounted in anti-fade with DAPI and sealed.

Laser scanning confocal microscopy of parasites and imaging controls. Confocal microscopy was performed using Nikon A1R microscope with diode (405 nm), argon (488 nm) and helium-neon green (543 nm), on parasites labeled for immunofluorescence using a 100X oil immersion lens. Images were viewed and analyzed using NIS elements software (version 3.2), which allows qualitative display of multiple colors from spatially over-lapping probes. These data were also analyzed from three dimensional overlaps based on Z-stacks of cells. To avoid inter-channel mixing (405 nm, 488 nm and 594 nm), pictures were captured separately with individual laser and were merged later. Pre-immune serum was used along with antigen specific antibodies in western blot assays. When probed with pre-immune sera no bands were observed on western blots of total parasite lysate proteins. Using the same, no fluorescence was observed either. The following immunofluorescence controls were also included: (1) slides treated with pre-immune serum (dilution same as for the related protein) and suitable secondary antibody for each sample (2) slides treated with secondary antibody alone and (3) slides treated with combinations of secondary antibodies.

Competitive immuno-flourescence assays. Competitive assays for antigen and assay specificity of rabbit anti-Ed-ARS and rabbit anti-Ed-TRS were performed in duplicates. Purified IgG was pre-incubated with equimolar and 10 fold molar excess of respective antigens prior to assays. In IFAs, ~400 nM of pre-incubated and control antibodies were used to address specificity of Ed-ARS and Ed-TRS antibodies.

Parasite growth inhibition assays using aaRS inhibitors. To assess the effect of selected inhibitors on malaria parasite growth *in vitro*, synchronous ring-stage 3D7 strain *P. falciparum* parasites were cultured in a 96-well plate with varying concentrations of different inhibitors for 48 h. The culture medium was then changed every day, maintaining appropriate concentration of inhibitors. *P. falciparum* proliferation in human erythrocytes was measured utilizing SYBR green I dye DNA staining assay, as described earlier[43]. After 48 h of growth, 100 µl lysis buffer containing SYBR Green I (.2 µl /ml of lysis buffer) was added to each well and contents were mixed until no visible erythrocyte sediment remained. After 1 h of incubation in dark at room temperature, fluorescence was using fluorescence multiwell plate reader (Victor3, Perkin Elmer) with excitation and emission wavelength bands centered at 485 and 530 nm respectively. Chloroquine was used as a positive control in all experiments. Stock solutions of chloroquine were prepared in water (milliQ grade) while aaRS inhibitors compounds were dissolved in DMSO. All stocks were then diluted with culture medium to achieve the required concentrations (in all cases the final concentration contained 0.2% DMSO, which was found to be non-toxic to the parasite). Drugs and test compounds were then placed in 96-well flat-bottom tissue culture grade plates to yield triplicate wells with drug concentrations ranging from 0 to 1 mM in a final well volume of 100 µl. The IC_{50} values were obtained by plotting fluorescence readings against drug concentration and by visual matching of inhibitor concentration giving 50% growth. To re-validate data and obtained more accurate IC_{50} values top compounds for each target protein were re-tested in an intra-plate titration format using seven points, and two fold dilutions of the compounds were used.

Cytotoxicity activity measurement. Animal cell lines (HeLa and fibroblast L929) were used to determine inhibitor toxicity by using MTT [3-(4,5-Dimethylthiazol-2-yl)-2,5-Diphenyltetrazolium Bromide] assay for mammalian cell viability[44]. HeLa and Fibroblast L929 cells were cultured in complete RPMI containing 10% fetal bovine serum, 0.2% sodium bicarbonate, 50 mg/ml gentamycin. Briefly, cells (104 cells/200 ml/well) were seeded into 96-well flat-bottom tissue-culture plates in complete culture medium. Drug solutions were added after overnight seeding and incubated for 24 h in a humidified atmosphere at 37°C and in 5% CO_2. DMSO (final concentration 10%) was added as positive control. An aliquot of stock solution of MTT (5 mg/ml in 1x phosphate-buffered saline) was added at 20 µl per well, and incubated for another 4 h. After spinning the plate at 1500 rpm for 5 min, supernatants were removed and 100 µl of the stop agent DMSO added. Formation of formazan (chromogenic product from MTT reduction) - an index of survival, was measured at 570 nm. The dose response curves of selected inhibitors in cytotoxic assay were analyzed for toxicity at parasite inhibitory concentration (IC_{50} values).

1. WHO World malaria report 2009. Geneva, Switzerland (2009).
2. Miller, L. H., Baruch, D. I. Marsh, K. & Doumbo, O. K. The pathogenic basis of malaria. *Int J. Parasitiol.* **405**, 673–679 (2002).
3. Ibba, M. & Soll, D. Aminoacyl-tRNA synthesis. *Annu Rev Biochem.* **69**, 617–50 (2000).
4. Jakubowski, H. Accuracy of aminoacyl-tRNA synthetases: proofreading of amino acids. In the Aminoacyl-tRNA Synthetases. ed. Ibba. M., Francklyn, C. & Cusack, S. pp. 354–96 *Austin, TX: LandesBiosci./Eurekah.com* (2005).
5. Ling, J., Reynolds, N. & Ibba, M. Aminoacyl-tRNA synthesis and Translational quality control. *Annu Rev Microbiol.* **63**, 61–78 (2009).
6. Bhatt, T. K., Bhatt, T. K., Yogavel, M., Wydau, S., Berwal, R. & Sharma, A. Ligand bound structures provide atomic snapshots for the catalytic mechanism of D-amino acid deacylase. *J. Biol Chem.* **285**, 5917–30 (2010).
7. Yogavel, M., Khan, S., Bhatt, T. K. & Sharma, A. Structure of D-tyrosyl-$tRNA^{Tyr}$ deacylase using home-source Cu Kα and moderate-quality iodide-SAD data: structural polymorphism and HEPES-bound enzyme states. *Acta Crystallogr D Biol Crystallogr.* **66**, 584–592 (2010).
8. Lee, J. W., Beebe, K., Nangle, L. A., Jang, J. & Longo-Guess, C. M. Editing-defective tRNA synthetase causes protein misfolding and neurodegeneration. *Nature.* **443**, 50–55 (2006).
9. Bhatt, T. K. *et al.* A genomic glimpse of aminoacyl-tRNA synthetases in malaria parasite *Plasmodium falciparum. BMC Genomics.* **10**, 644– 659 (2009).
10. Yunqing, L., Jing, L., Bin, B., Wang, E. D., Ding, J. Crystal structures of the editing domain of *Escherichia coli* leucyl-tRNA synthetase and its complexes with Met and Ile reveal a lock-and-key mechanism for amino acid discrimination. *Biochem J* **394**, 399–407 (2004).
11. Fukunaga, R., Yokoyama, S. Structural Basis for Substrate Recognition by the Editing Domain of Isoleucyl-tRNA Synthetase. *J. Mol. Biol.* **359**, 901–912 (2006).
12. Sokabe, M., Okada, A., Yao, M., Nakashima, T., Tanaka, I. Molecular basis of alanine discrimination in editing site. *Proc Natl Acad Sci USA.* **102**, 11669–74 (2005).
13. Dock-Bregeon, A. C., Rees, B., Torres-Larios, A., Bey, G., Caillet, J., Moras, D. Achieving error-free translation; the mechanism of proofreading of threonyl-tRNA synthetase at atomic resolution. *Mol Cell.* **16**, 375–86 (2004).
14. Istvan, E. S., Dharia, N. V., Bopp, S. E., Gluzman, I., Winzeler, E. A. & Goldberg, D. E. Validation of isoleucine utilization targets in Plasmodium falciparum. *Proc Natl Acad Sci USA.* **108**, 1627–32 (2011).
15. Zuegge, J., Ralph, S., Schmuker, M., McFadden, G. I. & Schneider, G. Deciphering apicoplast targeting signals-feature extraction from nuclear-encoded precursors of Plasmodium falciparum apicoplast proteins. *Gene.* **280**, 19–28 (2001).
16. Cokol, M., Nair, R. & Rost, B. Finding nuclear localization signals. *EMBO reports.* **1**, 411–415 (2000).
17. Schneider, A. Mitochondrial tRNA import and its consequences for mitochondrial translation. *Annu Rev Biochem.* **80**, 1033–53 (2011).
18. Guo, M., Chong, Y. E., Shapiro, R., Beebe, K., Yang, X. L. & Schimmel, P. Paradox of mistranslation of serine for alanine caused by AlaRS recognition dilemma. *Nature.* **462**, 808–12 (2009).
19. Kotik-Kogan, O., Moor, N., Tworowski, D. & Safro, M. Structural basis for discrimination of L-phenylalanine from L-tyrosine by phenylalanyl-tRNA synthetase. *Structure.* **13**, 1799–807 (2005).
20. Bacher, J. M., Crécy-Lagard, V. & Schimmel, P. Inhibited cell growth and protein functional changes from an editing-defective tRNA synthetase. *Proc Natl Acad Sci USA.* **102**, 1697–1701 (2005).
21. Nangle, L. A., Motta, C. M. & Schimmel, P. Global effects of mistranslation from an editing defect in mammalian cells. *Chem Biol.* **13**, 1091–1100 (2006).
22. Netzer, N. *et al.* Innate immune and chemically triggered oxidative stress modifies translational fidelity. *Nature.* **462**, 422–6 (2009).
23. Chaubey, S., Kumar, A., Singh, D. & Habib, S. The apicoplast of Plasmodium falciparum is translationally active. *Mol Microbiol.* **56**, 81–89 (2005).
24. Gardner, M. J. *et al.* Genome sequence of the human malaria parasite *Plasmodium falciparum. Nature.* **419**, 498–511(2002).
25. Liu, J., Istvan, E. S., Gluzman, I. Y., Gross, J. & Goldberg, D. E. Plasmodium falciparum ensures it's amino acid supply with multiple acquisition pathways and redundant proteolytic enzyme systems. *Proc Natl Acad Sci USA.* **103**, 8840–8845 (2006).
26. Karkhanis, A. V., Boniecki, T. M., Poruri, K. & Martinis, A. S. A Viable Amino Acid Editing Activity in the Leucyl-tRNA Synthetase CP1-splicing Domain Is Not required in the Yeast Mitochondria. *J. Biol Chem.* **281**, 33217–33225 (2006).
27. Lue, S. W. & Kelley, S. O. An aminoacyl-tRNA Synthetase with defunct editing site *Biochemistry.* **44**, 3010–3016 (2005).

28. Soutorina, J., Plateu, P., Delort, F., Peirotes, A. & Blanquet, S. Functional Characterization of the D-Tyr-tRNA^{Tyr} Deacylase from *Escherichia coli*. *J. Biol Chem.* **274**, 19109–14 (1999).
29. Ahel, I., Kroencic, D., Ibba, M. & Soll, D. Trans-editing of mischarged tRNAs. *Proc Natl Acad Sci USA.* **100**, 15422–15427 (2003).
30. Ibba, M. & Soll, D. Quality control mechanisms during translation. *Science.* **286**, 1893–97 (1999).
31. Bhal, A. *et al.* PlasmoDB: the Plasmodium genome resource. A database integrating experimental and computational data. *Nucleic Acid Res.* **31**, 212–5 (2003).
32. Altschul, S. F., Gish, W., Miller, W., Myers, E. W. & Lipman, D. J. Basic local alignment search tool. *J. Mol Biol* **215**, 403–10 (1990).
33. Wilson, D. *et al.* SUPERFAMILY-Comparative Genomics, Data mining and Sophisticated Visualisation. *Nucleic Acids Res.* **37**, 380–386 (2009).
34. Letunic, I., Doerks, T. & Bork, P. SMART 6 Recent updates and new developments. *Nucleic Acids Res.* **37**, 229–232 (2008).
35. Bateman, A. *et al*. The Pfam: protein families database. *Nucleic Acids Res.* **30**, 276–280 (2002).
36. Altschul, S. F. *et al.* Gapped BLAST and PSI-BLAST: a new generation of protein database search programs. *Nucleic Acids Res.* 25, 3389–3402 (1997).
37. Papadopoulos, J. S. & Agarwala, R. COBALT: constraint-based alignment tool for multiple protein sequences. *Bioinformatics.* **23**, 1073–79 (2007).
38. Eswar, N. *et al.* Comparative protein structure modeling using MODELLER. *Corr Protoc Protein Sci.* **50**, 2.9. 1–2.9.31 (2007).
39. Prime, version 3.0 Schrödinger, LLC, New York, NY (2011).
40. Trott, O. & Olson, A. J. AutoDock Vina: improving the speed and accuracy of docking with a new scoring function, efficient optimization and multithreading. *J. Comp Chem.* **31**, 455–461 (2010).
41. Lambros, C. & Vandenberg, J. P. Synchronization of Plasmodium falciparum erythrocytic stages in culture. *J. Parasitol.* **65**, 418–420 (1979).
42. Tonkin, C. J. *et al.* Localization of organellar proteins in Plasmodium falciparum using a novel set of transfection vectors and a new immunofluorescence fixation method. *Mol. Biochem. Parasitol.* **137**, 13–21 (2004).
43. Smilkstein, M., Sriwilaijaroen, N., Kelly, J. X., Wilairat, P. & Riscoe, M. Simple and Inexpensive Fluorescence-Based Technique for High-Throughput Antimalarial Drug Screening. *Antimicrob Agents Chemother.* **48**, 1803–1806 (2004).
44. Mosmann, T. Rapid colorimetric assay for cellular growth and survival: application to proliferation and cytotoxicity assays. *J Immuno Met.* **65,** 55–63 (1983).

Acknowledgments

SK, AS, AJ, AKP, KKT are supported by Department of Biotechnology and CSIR, Govt. of India. Amit Sharma acknowledges DBT, Govt of India for funding.

Author contributions

The following conceived and designed these experiments: SK, AS, AJ and AS. Experiments were performed and analyzed by: SK, AS, AJ and AS. The following contributed reagents/materials/analysis tools: AKP, KKT. SK, AS, AJ and AS wrote the paper. VS contributed to the manuscript writing.

Additional information

Supplementary information accompanies this paper at http://www.nature.com/scientificreports

Competing financial interests: The authors declare no competing financial interests.

How to cite this article: Khan, S. *et al.* Uneven spread of *cis*- and *trans*-editing aminoacyl-tRNA synthetase domains within translational compartments of *P. falciparum*. *Sci. Rep.* **1**, 188; DOI:10.1038/srep00188 (2011).